

# Pleading for a Dual Molecular-Orbital/Valence-Bond Culture

Philippe C. Hiberty\* and Benoît Braïda\*

bent bonds · hybridization · molecular orbital theory ·  
valence bond theory

## 1. Introduction

The origin of valence bond (VB) theory dates back to the landmark 1927 paper of Heitler and London,<sup>[1]</sup> which described the bonding in the H<sub>2</sub> molecule in terms of the pairing of the two electrons in the two atomic orbitals (AOs) and appeared as the quantum mechanical formulation of Lewis's electron-pair bonding. The generalization to polyatomic molecules was later achieved by Pauling,<sup>[2]</sup> Slater,<sup>[3]</sup> Wheland,<sup>[4]</sup> Eyring and Polanyi,<sup>[5]</sup> and their co-workers, and led to novel and fundamental concepts, such as hybridization, resonance, electronegativity, and provided a solid theoretical ground for other ubiquitous chemical concepts such as the arrow-pushing language in reactivity for instance. Those concepts allowed the rationalization of huge amounts of chemical observations by means of a few guidelines. In particular, the notion of orbital hybridization proved extremely useful and was used to discuss molecular geometries and bond angles in a variety of molecules, ranging from organic to transition metal compounds. VB theory was immediately adopted by chemists, who discovered a model that was close to the traditional notion of valence that viewed molecules as ensembles of atoms held together by local bonds.

About at the same time that VB theory was developed, Hund<sup>[6]</sup> and Mulliken<sup>[7]</sup> developed molecular orbital (MO) theory as an alternative approach, in which the electrons in a molecule occupy delocalized orbitals made from linear combinations of AOs. Yet, MO theory, with its delocalized orbitals that seemed alien to everything chemists had thought about the nature of the chemical bond, was not readily accepted by chemists whereas VB remained the most popular theory during the 1930–1950s.

By the mid-1950s, the tide started shifting slowly in favor of MO theory, gaining momentum through the mid-1960s. The first major impact was given by Hückel's rules,<sup>[8]</sup> which proved very useful to rationalize stability in  $\pi$  systems—cyclopropenyl cation, tropylium, cyclopentadienyl anion. Soon after, Walsh diagrams made a great impact on spectroscopists,<sup>[9]</sup> and the MO model was also found to be particularly well suited to predict spectra and electronic transitions. In the field of organic chemistry, the mechanisms of pericyclic reactions were elegantly elucidated with the publication of the MO-based Woodward–Hoffmann rules,<sup>[10]</sup> and the model of Fukui's frontier orbitals<sup>[11]</sup> proved successful to predict many aspects of chemical reactivity. Moreover, MO theory was naturally adapted to the study of extended materials whereas VB was not. Last but not least, the development of photoelectron spectroscopy and its application to molecules in the 1970s showed that the spectra could be easily interpreted as reflecting the energies of canonical molecular orbitals.<sup>[12]</sup> This experimental support was taken by many researchers and teachers as the decisive proof that MO theory was the only legitimate chemical theory of bonding. On the other hand, VB theory was claimed, on the basis of simplistic reasoning, to be unable to account for, for example, the two ionization potentials of methane or water or for the triplet ground state of dioxygen. Yet, although the falseness of such assertions (which, amazingly, keep appearing here and there even in some recent textbooks)<sup>[13]</sup> could easily be demonstrated on the back on an envelope<sup>[14]</sup> (see below), a fence of misunderstanding started to build up between two visions of molecules: the VB view that was close to the natural language of chemists, with the electron pairs located in local bonds or lone pairs, and the MO view with its electron pairs represented as completely delocalized over the whole molecule.

One consequence of MO theory taking the upper hand was some distrust about the concepts arising from VB, in particular hybridization, which was deemed wrong by some theoretical chemists and teachers. Despite this, chemists continued to widely use the hybridization concept, which easily explains molecular shapes as well as the transferabilities of specific and constant bond lengths, bonding energies, and vibrational frequencies of, for example, the C–H bonds in each of the alkane, alkene, and alkyne families. However, they were often feeling some vague guilt for using a concept that was not in the tool kit of the prevailing theory of bonding and was rejected by some theoreticians.

[\*] Prof. Dr. P. C. Hiberty  
Laboratoire de Chimie Physique, CNRS UMR8000, Bat. 349,  
Université de Paris-Sud  
91405 Orsay Cédex (France)  
E-mail: philippe.hiberty@u-psud.fr

Dr. B. Braïda  
Sorbonne Université, CNRS, Laboratoire de Chimie Théorique  
75005 Paris (France)  
E-mail: benoit.braïda@sorbonne-universite.fr

 The ORCID identification number(s) for the author(s) of this article can be found under:  
<https://doi.org/10.1002/anie.201710094>.

Such was the situation up to the 1980s, when VB theory started to make a strong come back, mainly because of the emergence of qualitative and semi-quantitative applications of VB theory to a variety of chemical and biochemical problems.<sup>[15]</sup> Another factor that favored the VB renaissance was the development of new methods for ab initio VB calculations<sup>[16–19]</sup> and the availability of efficient and user-friendly software with fast algorithms.<sup>[20,21]</sup> It was then found that high-level VB calculations could yield accurate results in terms of energies and all kinds of molecular properties, just like MO calculations followed by extensive configuration interaction (CI). Moreover, even qualitative concepts arising from VB such as resonance energy, interacting Lewis structures, hybridization and so on, could be numerically tested and given quantitative support. As an example among many others, the hybridization model was convincingly supported by Gerratt et al., who showed in 1988 that the most general and lowest-energy wave function that describes the electronic structure of methane, as a single configuration with fixed orbital occupancies, takes the form of four equivalent  $sp^3$  hybrids, each being singlet-coupled to a hydrogen AO.<sup>[22]</sup> Last but not least, a powerful general reactivity model, based on valence bond state correlation diagrams and aimed at rationalizing/predicting the magnitudes of reaction barriers from properties of reactants, started to be developed by Shaik et al. and ended up as a unified system of thought of the fundamentals of reactivity and reaction mechanisms.<sup>[23]</sup>

Today, it is fair to say that MO and VB theories are largely accepted as being both correct, even if MO-CI remains by far the most often used one in calculations, mainly for computational-cost reasons, whereas ab initio VB calculations are appreciated as providing much more compact wave functions for the same accuracy<sup>[24]</sup> and for their natural ability to calculate diabatic states. On the other hand, what is still often missing, we believe, is a real dual MO/VB culture, that is, the recognition that both theories are equally valid from both the qualitative and computational points of view; and more generally, that the delocalized and localized pictures of the electron pairs are also equally valid, despite the apparent paradox. In addition, the knowledge of the bridges that allow one to switch from one description to the alternative one is very helpful to getting a complete view of the electronic structure of a molecular state, as the localized view might highlight one factor in bonding better than the delocalized one whereas the reverse might be true for another factor.

The aim of this paper is to familiarize the reader with the basic principles of the VB method, and to show, by means of illustrative examples, the usefulness of the simplest bridges among the many ones that have been devised so far<sup>[25–31]</sup> to connect the delocalized pictures to the localized ones.

## 2. Basic Principles of Classical Valence Bond Approach by Modern Methods

The VB wave function that we refer to in this paper is a multistructure one,  $\Psi_{VB}$ , which is expressed as a linear combination of Heitler–London–Slater–Pauling functions,  $\Phi_K$ , in Equation (1):

$$\Psi_{VB} = \sum_K C_K \Phi_K \quad (1)$$

where  $\Phi_K$  correspond to classical VB structures, and  $C_K$  are the corresponding structural coefficients. An important feature of this method is that all the active orbitals, that is, those that have varying occupancies in the VB structures, are strictly localized on a single atom, so as to ensure a clear correspondence between the mathematical expressions of the VB structures and their physical meaning, for example, displaying covalent or ionic bonds. Of course, such strictly localized AOs are non-orthogonal. Other non-orthogonal VB methods exist, using semi-localized atomic orbitals<sup>[32]</sup> but are not discussed in this paper.

The coefficients  $C_K$  in Equation (1) are determined by solving the usual secular equation  $HC = EMC$ , where Hamiltonian and overlap matrix elements are defined as in Equations (2) and (3), respectively:

$$H_{KL} = \langle \Phi_K | \hat{H} | \Phi_L \rangle \quad (2)$$

$$M_{KL} = \langle \Phi_K | \Phi_L \rangle \quad (3)$$

In the VBSCF method of van Lenthe and Balint-Kurti,<sup>[16]</sup> both VB orbitals and structure coefficients are simultaneously optimized to minimize the total energy, in strong analogy with the CASSCF method in the MO framework. As MO configurations and VB structures span the same space of configurations, the secular equations in the MO-CASSCF or VBSCF framework, at this level of calculation, must lead to nearly equivalent wave functions, albeit expressed in different forms. Indeed, a full-valence CASSCF calculation, for example a 8-electron-8-orbital calculation on methane, contains the same number of configurations as a full-valence VBSCF calculation on the same molecule (1764), and both methods provide the totality of static electron correlation, whatever the basis set of orbitals that is used. To summarize, the coefficient and the energy of a VB structure in a VBSCF calculation are as reliable as the coefficient and energy of an MO configuration in a MO-based CASSCF.

## 3. Unitary Transformations in a Slater Determinant: A Bridge between Delocalized and Localized Pictures

The standard MO wave function involves canonical MOs (CMOs), which are permitted to delocalize over the entire molecule. However, it is well known<sup>[25]</sup> that replacing two orbitals by their sum and difference, or more generally making any unitary transformations of the orbitals, in a Slater determinant keeps its total value rigorously unchanged and hence leaves the corresponding many-electron wave function invariant, yielding the same energy, electronic density, and molecular properties as the original one based on CMOs. If the unitary transformations are performed so as to comply with a criterion of minimal repulsion between electron pairs, the so-transformed orbitals appear as localized MOs (LMOs), known also as localized bond orbitals (LBOs). The equiv-

alence between CMO-based and LBO-based determinants is expressed in Equation (4):

$$\left| \dots \phi_i^{\text{cmo}} \dots \phi_j^{\text{cmo}} \dots \right| = \left| \dots \phi_i^{\text{lbo}} \dots \phi_j^{\text{lbo}} \dots \right| \quad (4)$$

These LBOs, which reveal an electronic molecular structure made of electron pairs each localized on a single atom (lone pairs) or between two atoms (bonds), have an obvious relationship to the Lewis structures that have been used by chemists to describe molecules for a century. For example, the central atom of methane is found to display four  $sp^3$  hybrid atomic orbitals (HAOs), pointing in tetrahedral directions and each linked to the 1s atomic orbital of a hydrogen, quite like the picture of methane arising from a VB calculation by Gerratt<sup>[22]</sup> (see above). Similarly, alkenes and alkynes exhibit local electron pairs in LBOs involving  $sp^2$  and  $sp$  HAOs, respectively, uniquely defined at the Hartree–Fock level and free of any a priori assumption. This clearly shows that the localized representation of electron pairs and Lewis structures are already present at the localized Hartree–Fock level in MO theory.<sup>[25]</sup> Today, thanks to the possibility for anyone to get well-defined HAOs by just pressing a button using modern chemistry software, the hybridization concept is generally accepted, despite rare exceptions.<sup>[33,34]</sup>

Of course, the localization of orbitals by unitary transformations can be applied to lone pair orbitals as well as bonding ones. This leads us to the much debated question of the rabbit-ear lone pairs of  $H_2O$ .

### 3.1. What Are the “Real” Lone Pairs of $H_2O$ ?

Two representations are popular for the lone pair orbitals of the water molecule: 1) The “rabbit-ear” orbitals, which are two equivalent HAOs, approximately of  $sp^3$  type and making an angle of circa  $112^\circ$ ,<sup>[14b]</sup> one above and one below the molecular plane ( $h_u$  and  $h_d$  in Figure 1) and 2) the CMOs, respectively of  $\sigma$  and  $\pi$  types, which are non-equivalent ( $n$  and  $p$  in Figure 1). The rabbit-ear orbitals  $h_u$  and  $h_d$  are nothing else than the sum and difference of the  $n$  and  $p$  CMOs.

Two opposite commonly used arguments support one representation or the other:

- The oxygen atom of water may form two equivalent hydrogen-bonds with neighboring molecules, for example, with other water molecules in ice. Now a hydrogen-bond is not only an electrostatic interaction but is also partially covalent, and therefore displays some bonding orbital interaction between a lone pair orbital of oxygen and the 1s orbital of the neighboring hydrogen.<sup>[35]</sup> Since the two hydrogen-bonds are equivalent, the lone pair orbitals that are involved in these bonds should also be equivalent.
- The photoelectron spectrum of water shows two different ionization peaks, which correspond fairly well to the respective energies of the  $\pi$  and  $\sigma$  CMOs,  $p$  and  $n$  in Figure 1. Assuming that one gets ionized water by simply taking off an electron from one of its lone pair orbitals, the lone pair orbitals must be non-equivalent and therefore be the CMOs rather than the rabbit-ears.

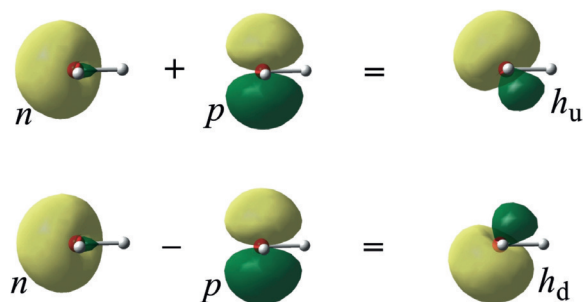


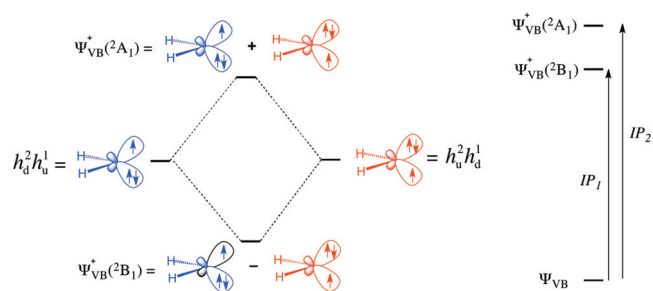
**Figure 1.** Canonical orbitals for the lone pairs of  $H_2O$  ( $n, p$ ) and equivalent localized rabbit-ear orbitals resulting from their sum and difference ( $h_u, h_d$ ).

It is undeniable that the non-equivalent  $\sigma$ – $\pi$  CMOs are a valid orbital set for the lone pairs of water, since they directly arise from a standard Hartree–Fock calculation whose many-electron wave function reproduces the molecular properties fairly well. It is also undeniable that applying a localization procedure, through unitary orbital transformations,<sup>[25]</sup> provides two equivalent lone pair orbitals of quasi- $sp^3$  type (see Figure 1), making an angle of  $112^\circ$  very close to the angle  $114^\circ$  between the two hydrogen bonds made by the oxygen atom in ice,<sup>[14b]</sup> and we know that this orbital set provides exactly the same many-electron wave function as the CMO set. It follows that the rabbit-ears also provide a valid set of lone pair orbitals for water, just like the  $\sigma$ – $\pi$  CMOs! Why, then, are there two distinct ionization potentials for water? To answer this question, one must re-examine the argument that is so often used to declare the rabbit-ears invalid.

This argument is based on the supposition that one gets the picture of ionized water just by removing one electron from a lone pair orbital. While this is true in the CMO representation, in which the orbitals are symmetry-adapted, this is not true in the localized representation. Indeed, simply removing an electron from one of the localized lone pairs leads to either the  $h_d^2 h_u^1$  or the  $h_u^2 h_d^1$  configuration (respectively in blue and red in Scheme 1) but neither of these VB structures may represent, by itself, ionized water because neither matches the symmetry of the molecule. Thus, a correct representation of ionized water must be a combination of  $h_d^2 h_u^1$  and  $h_u^2 h_d^1$ , and not any one of these functions alone. Now there are two possible combinations, one positive and the other negative, respectively leading to the correct high-lying  ${}^2A_1$  and low-lying  ${}^2B_1$  ionized states, thus accounting for the two distinct ionization potentials.

Note that the two ionization potentials  $IP_1$  and  $IP_2$  of Scheme 1, which are obtained with the rabbit-ear representation, are quantitatively exactly the same as the ionization potentials obtained in the CMO framework, as the energies of the  $n$  and  $p$  CMOs of Figure 1.<sup>[36]</sup>

Finally, back to the subsection title question, what are the real lone pair orbitals of  $H_2O$ ? This question has actually no answer, as it implies the fundamentally wrong assumption that orbitals would be some real, uniquely existing objects that could possibly be experimentally observed, just like, for example, electron densities, dipole moments, and so on. As



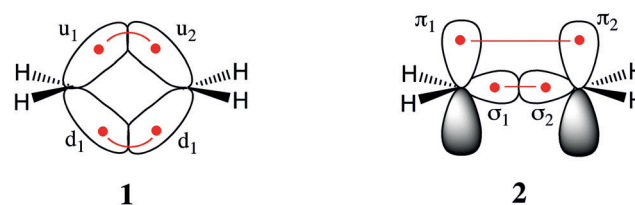
**Scheme 1.** Construction of the two ionized states of water in the valence bond framework with rabbit-ear lone pair orbitals.

has been recently reaffirmed,<sup>[37]</sup> this is obviously not the case, since orbitals are neither unique nor observable, as molecular energy and density are invariant to unitary orbital transformations within a given subspace, as has been recalled above.

Now, a slightly different question might be, “What is the best (chemically speaking, that is, more insightful or more convenient than another depending on which chemical property one wishes to illustrate or compute) orbital set to describe a given molecule?” For example, to obtain an orbital set that best shows how some electron pairs arrange themselves in 3D space, one can use a physical criterion of minimal repulsion between electron pairs,<sup>[25]</sup> which will provide, for example, a set of LMOs with two rabbit-ear lone pair orbitals in the case of H<sub>2</sub>O. As we will see in section 5, this is precisely the image that is also retrieved by density map analyses and by different sophisticated modern interpretative methods aiming at answering the very same question of how electrons and electron pairs are located in real space. In turn, the CMOs are the only orbitals that are eigenfunctions of an electron in the averaged-field of the others and as such have a direct connection with the ionization potentials (IPs) within both HF and KS-DFT theories.<sup>[38]</sup> Thus, taking the water molecule as an example, the two distinct IPs can be simply estimated, to a good approximation, as the respective energies of the two highest-lying CMOs. Of course, the very same distinct IPs can also be obtained within the rabbit-ear orbital representation (see above and Scheme 1) but in a far less elegant way. Conversely, the orbital interactions of the two equivalent hydrogen bonds attached to a water molecule are elegantly addressed by using the equivalent rabbit-ear orbitals, whereas using the CMO ones necessitates more complicated reasoning and calculations.

### 3.2. The $\sigma$ - $\pi$ Bonds versus Bent Bonds of Ethylene

The ethylene molecule was first described by Pauling as forming a C=C bond between two CH<sub>2</sub> units by means of tetrahedral hybrids, giving rise to two bent bonds having the shapes of bananas (hence the term “banana bonds”), one above and the other below the molecular plane (**1** in Scheme 2).<sup>[2]</sup> On the other hand, the  $\sigma$ - $\pi$  separation, which naturally arises from the symmetry properties of the CMOs, was used by Hückel<sup>[8]</sup> as early as 1931, primarily as a mean to

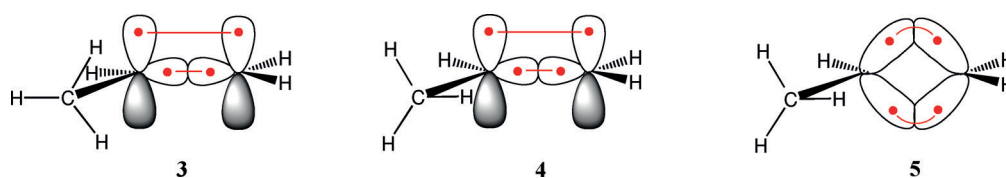


**Scheme 2.** The C-C bonding orbitals in the bent-bond representation (**1**) and in the canonical  $\sigma$ - $\pi$  representation (**2**).

tackle a many-electron problem in ethylene or conjugated molecules by considering only the  $\pi$ -electrons explicitly, while incorporating the rest in an effective Hamiltonian. This notion has led to fundamental concepts such as conjugation, aromaticity, anti-aromaticity, and ring currents. In this model, the properties of conjugated systems are governed by two distinct sets of bonds,  $\sigma$  and  $\pi$ . The  $\sigma$  bonds of conjugated molecules behave as sets of local two-electron bonds. On the other hand, because each  $\pi$ -AO can overlap with more than one neighbor,  $\pi$  systems exhibit electronic delocalization, which is at the origin of many of their special properties.<sup>[39]</sup>

Back to ethylene, the former model of bent bonds is rarely used in practice, although it is clear that both this model and the  $\sigma$ - $\pi$  ones are quantitatively equivalent from the standpoint of MO theory and interconvertible by unitary transformations of the MOs. Indeed, very simple algebra immediately shows that the sum and difference of the  $\sigma$  and  $\pi$  MOs of ethylene, ( $\sigma_1 + \sigma_2$ ) and ( $\pi_1 + \pi_2$ ) in **2** (Scheme 2), yield up and down combinations of banana types, ( $u_1 + u_2$ ) and ( $d_1 + d_2$ ) as in **1**. Remarkably, the  $\sigma$ - $\pi$ /bent-bond equivalence fairly carries over to electron-correlated ab initio computational levels, as shown by Messmer et al.<sup>[40]</sup> For triply bonded systems like C<sub>2</sub>H<sub>2</sub> or N<sub>2</sub>, analogous unitary transformations would lead to three equivalent bent bonds, forming a cage around the central axis. Again, “What are the best orbitals between the  $\sigma$ - $\pi$  and bent-bond representations?” is a meaningless question if one does not specify what is the property of interest; for instance, the  $\pi$  orbitals yield close-lying frontier orbitals and as such are the ones to use to apply this reactivity model. Moreover, the  $\sigma$ - $\pi$  separation allows one to characterize ring currents, aromatic stabilization, and so on in large conjugated systems. Thus, the  $\sigma$ - $\pi$  model gained wide adoption and amply proved its usefulness. On the other hand, the bent bonds better describe how the two bonding electron pairs are located in space, as will be seen in Section 4 in more details, and it turns out that this latter model is the most insightful one in a number of cases and has practical applications, like the conformational analysis of unsaturated acyclic systems.<sup>[2,41]</sup>

Indeed, a fundamental aspect of the bent-bond model is that it confers tetrahedral character to unsaturated carbons, including those in olefins and carbonyl compounds, and allows one to apply conformational analysis in the same way as with saturated systems. Let us consider the propene molecule as an example (Scheme 3) and look for the preferred conformation of the methyl group. Do the hydrogens of the methyl group prefer to eclipse the vinylic hydrogen as in **3** or the double bond as in **4**? The answer is not so intuitive if one considers the C=C bond in the  $\sigma$ - $\pi$



**Scheme 3.** Conformations of propene in the  $\sigma$ - $\pi$  representation (3, 4) and in the bent-bond representation (5).

representation. Perhaps a C=C bond is more bulky than a single C–H bond, in which case conformation **3** would be preferred? But conformation **4** is found to be the most stable one experimentally, and the reason why it is so is not self-evident considering  $\sigma$ - $\pi$  orbitals. However, representing the C=C bond with bent bonds as in **5**, immediately gives the answer: The best conformation is **4**, or equivalently **5** in the framework of bent bonds, because in the latter model one can see that all the hydrogens of methyl are staggered relative to the tetrahedral bonds of the adjacent vinyl group. Thus, the problem becomes as simple as finding the best conformation of, for example, ethane. Accordingly, **4** is found to lie  $1.97 \text{ kcal mol}^{-1}$  below **3** at the CCSD(T)/aug-cc-pVQZ computational level (this work, on geometries optimized at the CCSD/cc-pVTZ level). The same model is successfully applied to substituted carbonyl groups, vinyl ethers, acetaldehyde, propionaldehyde, enol ethers, enamines, and so on.<sup>[41]</sup>

#### 4. Invariance of a CASSCF Wave Function to Unitary Transformations: Application to the $C_2$ Molecule

The invariance of a wave function under unitary transformation of its orbitals is not limited to single determinants but extends to CASSCF wave functions. This property can be used to transform a CASSCF wave function based on CMOs so as to get more insight on the nature of bonding in a molecule, as will be exemplified below with the controversial  $C_2$  molecule, whose electronic structure has been fiercely debated.<sup>[42–45]</sup> Can we clearly visualize the bonding nature of this little molecule and relate it to its essential feature, its avid reactivity?

The CMOs arising from a CASSCF(8,8) calculation of  $C_2$  are shown in Figure 2a. It is seen that the major configuration is the Hartree–Fock one, with a minor contribution of the  $2\sigma_u \rightarrow 3\sigma_g$  double excitation. Considering only the major configuration, since the  $2\sigma_g$  orbital is bonding whereas  $2\sigma_u$  is antibonding, a very crude reasoning might lead to the conclusion that both these doubly occupied orbitals cancel one another, resulting in little or no  $\sigma$ -bonding at all as in **6** (Scheme 4), whereas any  $\sigma$ -bonding would arise from the  $2\sigma_u \rightarrow 3\sigma_g$  configuration, with a weight of only 13.6%.<sup>[42j]</sup>

A seemingly more elaborate method would consist of using the CMOs and their occupation numbers in a CASSCF calculation to estimate effective bond orders (EBOs) defined as in Equation (5):<sup>[42g]</sup>

$$EBO = \left( \sum n_{\text{bonding}} - \sum n_{\text{antibonding}} \right) / 2 \quad (5)$$

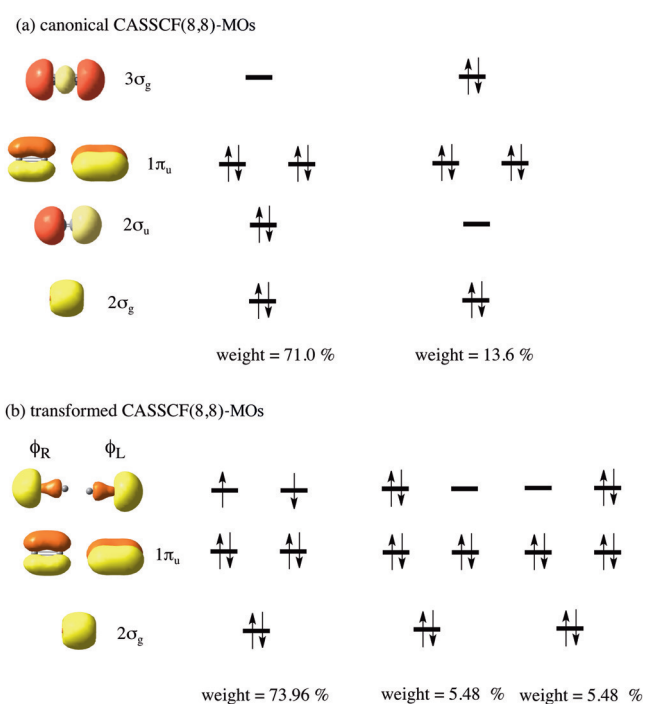
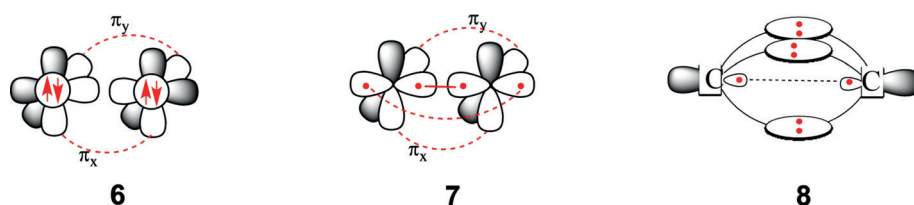


**Figure 2.** Orbitals, leading configurations of  $C_2$  and their respective weights, in: a) A standard full-valence CASSCF/6-31G\* wave function and b) the equivalent full-valence CASSCF wave function after unitary transformations of the  $2\sigma_u$  and  $3\sigma_g$  orbitals. The authors are thankful to M. Zhang, D. Danovich, and S. Shaik for permission to reproduce this figure.

where  $n$  stands for the occupation numbers of the CMOs. However, this definition, which looks reasonable, has the severe drawback of missing the quantitative magnitude of the bonding/antibonding character of the CMOs, and it turns out that this defect is particularly misleading in the case of  $C_2$ . Indeed, a simple inspection of the  $2\sigma_u$  MO, in Figure 2a, shows that this orbital, an out-of-phase combination of two lobes pointing away from each other, is very weakly antibonding, whereas the  $2\sigma_g$  one is strongly bonding. This is confirmed by the calculated overlap populations in these two MOs, 0.416 for  $2\sigma_g$  versus  $-0.076$  for  $2\sigma_u$  in cc-pVTZ basis set.<sup>[42h]</sup> Even worse, the overlap population in  $2\sigma_u$  flips from  $-0.025$  to a slightly positive value of  $+0.014$  as one goes from cc-pV5Z to cc-pV6Z, thus becoming formally bonding, and being considered as such in Equation (5) would therefore yield completely different values as the basis set is slightly changed! Clearly then, the ambiguous character of the  $2\sigma_u$  MO prevents the use of EBO for measuring the bond multiplicity. There are other definitions of bond orders, of



**Scheme 4.** Structure **6** is the doubly  $\pi$ -bonded structure of  $C_2$  that one would get if one assumed that the  $2\sigma_u$  and  $3\sigma_g$  CMOs cancel each other and result in practically no  $\sigma$ -bonding at all. Structure **7** is a quadruply bonded structure revealed by a unitary transformation of a CASSCF(8,8) wave function. Structure **8** is the same structure with bent bonds, appearing after a further transformation of the CASSCF wave function.

course, but they lead to a rather wide spectrum of values, ranging from 2.2 to 3.9.<sup>[42h]</sup>

It follows that standard CASSCF calculations with CMO-based wave functions are not of great help to determine the bonding nature of  $C_2$ . Now it has been shown by Zhang et al.<sup>[43]</sup> that using a unitary orbital transformation of some orbitals in a CASSCF(8,8) wave function leads to a much clearer picture. The unitary transformation simply consists of taking the sum and difference of the CMOs  $2\sigma_u$  and  $3\sigma_g$ , leading to the new orbitals  $\phi_L$  and  $\phi_R$  as in, dropping the normalization factors, Equation (6):

$$\varphi_L = 2\sigma_u + 3\sigma_g \quad (6a)$$

$$\varphi_R = 2\sigma_u - 3\sigma_g \quad (6b)$$

Of course, this time the determinants are not individually invariant, since we have mixed orbitals that have variable occupancies depending on the configurations, and their coefficients also change along with the transformation. However the overall CASSCF wave function, as well as its energy, remains unchanged. The so-transformed CASSCF wave function, equivalent to the standard one based on CMOs, is displayed in Figure 2b. The picture is now clearer: Three doubly occupied strongly bonding MOs, the unchanged  $2\sigma_g$  and  $1\pi_u$  ones, and two purely local HAOs  $\phi_L$  and  $\phi_R$ , pointing away from each other. In the major configuration, these two latter orbitals are singly occupied and coupled to a singlet, thus forming a purely covalent bond. The two other configurations of Figure 2b, with either  $\phi_L$  or  $\phi_R$  being doubly occupied, represent the two minor ionic components of the same bond. We are thus left with a picture of  $C_2$  displaying a triple bond, made of one  $\sigma$  and two  $\pi$  internal bonds like in acetylene, plus a fourth  $\sigma$  bond, linking together two external hybrids, and presumably weak due to the orientation of the HAOs (**7** in Scheme 4). All in all, the picture of  $C_2$  displaying a quadruple bond represents 84.9% of the CASSCF(8,8) wave function. Of course, the quadruply bonded structure can also be called a triple bond plus a weaker fourth “*exo*” bond or a triply bonded diradical stabilized by singlet coupling between the radical centers, depending if one wishes to consider a bond strength of 15–20 kcal mol<sup>-1</sup> sufficient to qualify as a bond. But all these denominations recover the same picture that fully explains the high reactivity of  $C_2$ , which reacts extremely fast with methane, alkenes, vinyl

acetylene, and so on;<sup>[42b]</sup> whether this is due to the ease of breaking the fourth bond or to the diradical character of  $C_2$  is immaterial.

Remarkably, the transformed CASSCF wave function of Zhang et al.<sup>[43]</sup> provides a bonding picture of  $C_2$  in full agreement with the direct VB calculations, which find the quadruply bonded structure **7** to be the major one and to lie 129.5 kcal mol<sup>-1</sup> below the structure **6** exhibiting two  $\pi$  bonds and no  $\sigma$  bonds.<sup>[42h]</sup> The VB calculation

further allows calculating the strength of the fourth bond, estimated to 15–20 kcal mol<sup>-1</sup>.<sup>[42e]</sup>

Did we now get all possible insight for the  $C_2$  molecule? Not quite yet. This picture **7** of two  $\pi$  bonds accompanied by two  $\sigma$  bonds sharing the same region of space along the C–C axis is not so easy to visualize. Isn't there some space conflict between the two  $\sigma$  bonds? The dilemma can be resolved by again appealing to a unitary orbital transformation. In the same way as the  $\sigma$  bond and two  $\pi$  bonds can be transformed into a set of three equivalent bent bonds in acetylene, we can mix the  $2\sigma_g$  and  $1\pi_u$  CMOs of  $C_2$  to get a cage made of three equivalent bent bonds leaving plenty of space for the fourth bond to establish spin coupling between  $\phi_L$  and  $\phi_R$  along the C–C axis, as shown in structure **8** in Scheme 4. Thus,  $C_2$  is a typical case illustrating the VB/MO equivalence and the interest of playing with unitary transformations: While the picture given by standard CMO-based CASSCF is unclear, adding and subtracting some  $\sigma$  CMOs gives a clearer picture, and finally a crystal-clear one is obtained by further transforming the  $\sigma$ – $\pi$  bonding CMOs to bent bonds.

## 5. Where Are the Electron Pairs Located in Real Space?

Contrary to orbitals, which are non-unique as has been recalled above,<sup>[25]</sup> the map of electron density in 3D space is a physical and observable property and is therefore quite unique. Moreover, one may also wonder in what region of space one has the maximum probability of finding an electron pair, and this also must be a unique property of the molecule. This specific question can be answered using the maximum probability domains of Savin et al.<sup>[46]</sup> Other recent advanced interpretative methods also aim at directly extracting an image of how the electrons and electron pairs arrange in real space.<sup>[44,45]</sup> With the help of all these practical tools, it is interesting to compare the actual location of electron pairs with the localized and delocalized orbital representations.

### 5.1. Electron Density Maps of Water and Acetylene

The electron density maps of water and acetylene are well documented and available on the internet.<sup>[47]</sup> For water, the density maxima associated with lone pairs precisely follow the

shapes of the rabbit-ear orbitals, which are obtained from Hartree–Fock theory after unitary transformations of the CMOs following localization procedures.<sup>[25]</sup> For ethylene, density maxima are found on both sides of the C–C axis, in compliance with the bent-bond orbitals that one obtains after unitary transformations of  $\sigma$  and  $\pi$  CMOs. It is to be noted that these density maps keep the same shape independently of the computational method that has been used to calculate the wave functions, Hartree–Fock with CMOs, CASSCF, density functionals, and so on.

### 5.2. Maximum Probability Domains

Savin et al. proposed to analyze a wave function by looking at the distribution of probabilities to find a given number  $\nu$  of electrons in some regions and all other  $N-\nu$  electrons outside of this domain.<sup>[46]</sup> Thus, extracting from a wave function the regions that maximize the probability to find 2 and only 2 electrons into it, called maximum probability domains (MPDs), gives us a rigorous probabilistic definition of the location of electron pairs in 3D space.

We have applied the MPD method to the wave functions of three molecules: Water, ethylene, and  $C_2$ , at the Hartree–Fock level (thus displaying delocalized CMOs) in cc-pVTZ triple-zeta basis set. The results are displayed in Figure 3,

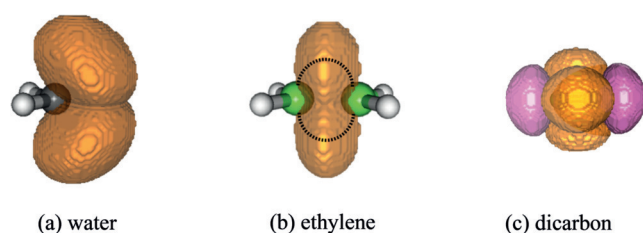


**Figure 3.** Some maximum probability domains for finding one and only one electron pair in water, ethylene, and dicarbon.

showing some regions that maximize the probabilities of finding a pair of electrons of opposite spins. For water and ethylene (Figure 3a,b), the results are quite similar to the well-known density maps (see previous subsection), or to the isosurfaces of the LMOs/LBOs. The water molecule displays two equivalent lone pairs having the shapes of rabbit-ears. For ethylene, the probability of finding an electron pair has two maximum domains on both sides of this axis, quite in agreement with the bent-bond model. Finally, the MPD calculations provide a very clear picture for the  $C_2$  molecule (Figure 3c), with three bent bonds forming a cage around the C–C axis (yellow domains), and two single-electron pink domains having the shapes of outward-directed hybrids, as is found in VB calculations or unitary-transformed CASSCF wave functions (**8** in Scheme 4). Note that a connection between the MPD method and VB theory has been recently emphasized.<sup>[48]</sup>

### 5.3. Maxima of the Squared Wave Function and Dynamic Voronoi Metropolis Sampling

Searching for the maxima of the square of the wave function, as originally proposed by Artmann, is another method that allows one to retrieve meaningful sets of electron arrangements into real space.<sup>[49]</sup> From these electron configurations, single electron densities can also be obtained, making chemical motifs appears, such as core electrons, lone pairs, and bonds. The dynamic Voronoi Metropolis sampling (DVMS) is another very recent method that also enables one to extract chemical motifs from accurate wave functions.<sup>[44]</sup> Both methods reveal two equivalent rabbit ears as the lone pairs of water as well as two bent bonds for ethylene. The DVMS method also reveals a triple bent-bonded structure for the  $N_2$  molecule and when applied to  $C_2$  arrives at an interpretation of its bonding in terms of a near triple bond (actually three bent bonds) with singlet-coupled outer electrons, quite equivalent to the MPD picture and to the VB and unitary-transformed CASSCF ones.

## 6. Conclusions

Molecular orbital theory and valence bond theory are equally valid and, if applied at the same level of sophistication, are only two ways of diagonalizing the same Hamiltonian in two different basis sets of configurations/structures, as was recognized as early as 1935 by van Vleck and Sherman.<sup>[50]</sup> MO-CI expresses the wave function in terms of symmetry-adapted MO configurations based, most of the time, on delocalized MOs and is best adapted to spectroscopy considerations, although chemical insight could be extracted when using fragment approach and/or energy decomposition analysis.<sup>[51]</sup> On the other hand, VB expresses the wave function in terms of VB structures, which are the quantum mechanical representations of Lewis structures with their local bonds and lone pairs, and is best adapted to the description of the nature of bonding in a molecule. Yet, both methods yield the same wave function, albeit expressed in different languages. Moreover, the delocalized/localized alternative already exists in the very framework of MO theory, since localized MOs can be obtained through unitary transformations, which leave Slater determinants invariant. More generally, there is an infinity of mathematically equally legitimate orbital sets that can be used to construct a given Slater determinant or Hartree–Fock wave function, and all of these sets provide the same wave function, electron density, dipole moments, net charges, Mulliken populations, and all measurable properties of a molecule. Thus, there exists nothing such as “the real orbitals” of a molecule, only orbital sets that are more insightful for a molecular property or another. This is well illustrated with the example of the water molecule, in which the energies of the CMOs immediately give the two distinct ionization potentials, whereas the localized rabbit-ear lone pair orbitals correctly give the directions of the two equivalent hydrogen bonds that the oxygen atom may form with its neighbors. Now, if the orbitals are not unique, the electron density and location of the

electron pairs in 3D space are unique, and these are closer to the localized representation than to the delocalized one.

Even if the VB and MO-CI theories, as well as the delocalized and localized orbital representations are all valid, the examples treated in this work show that it is very useful to possess both cultures and to understand when and why one vision may be more suitable than the other, as the bonding nature of a molecule may be totally blurred in one representation and become crystal clear in the other. Fortunately, transforming an MO-CI wave function or transforming delocalized MOs to localized ones is usually an easy task, either by means of standard software or possibly even by hand on the back of an envelope.

## Acknowledgements

Professor Wei Wu and his team are gratefully acknowledged for making their XMVB ab initio valence bond program available to us. We are thankful to Professor Sason Shaik and David Danovich for permission to use CASSCF data from Ref. [42h].

## Conflict of interest

The authors declare no conflict of interest.

**How to cite:** *Angew. Chem. Int. Ed.* **2018**, *57*, 5994–6002  
*Angew. Chem.* **2018**, *130*, 6100–6109

- 
- [1] W. Heitler, F. London, *Z. Phys.* **1927**, *44*, 455.  
 [2] L. Pauling, *The Nature of the Chemical Bond*, 3rd ed., Cornell University Press, Ithaca, **1960**.  
 [3] J. C. Slater, *Phys. Rev.* **1930**, *35*, 509–529.  
 [4] G. W. Wheland, *Resonance in Organic Chemistry*, Wiley, New York, **1955**.  
 [5] H. Eyring, M. Polanyi, *Z. Phys. Chem.* **1931**, *B12*, 279–311.  
 [6] a) F. Hund, *Z. Phys.* **1928**, *51*, 759–795; b) F. Hund, *Z. Phys.* **1931**, *63*, 719–751.  
 [7] R. S. Mulliken, *Phys. Rev.* **1932**, *41*, 49–71.  
 [8] a) E. Hückel, *Z. Phys.* **1931**, *70*, 204–286; b) E. Hückel, *Z. Phys.* **1932**, *76*, 628–648; c) E. Hückel, *Trans. Faraday Soc.* **1934**, *30*, 40–51.  
 [9] A. D. Walsh, *J. Chem. Soc.* **1953**, 2260–2331.  
 [10] R. B. Woodward, R. Hoffmann, *The Conservation of Orbital Symmetry*, Chemie, Weinheim, **1971**.  
 [11] K. Fukui, T. Yonezawa, H. Shingu, *J. Chem. Phys.* **1952**, *20*, 722–725.  
 [12] E. Heilbronner, H. Bock, *The HMO Model and its Applications*, Wiley, New York, **1976**.  
 [13] a) C. E. Housecroft, A. G. Sharpe, *Inorganic Chemistry*, 4th ed., Pearson, Harlow, **2012**, p. 34; b) G. Rayner-Canham, T. Overton, *Descriptive Inorganic Chemistry*, 6th ed., W. H. Freeman, **2014**, p. 530; c) B. W. Pfennig, *Principles of Inorganic Chemistry*, Wiley, Hoboken, **2015**, p. 271, p. 277.  
 [14] About the hybridization model, see a) P. C. Hiberty, F. Volatron, S. Shaik, *J. Chem. Educ.* **2012**, *89*, 575–577; b) P. C. Hiberty, D. Danovich, S. Shaik, *Chem. Educ. Res. Pract.* **2015**, *16*, 689–693. About the triplet state of dioxygen, see: P. C. Hiberty, S. Shaik, *Helv. Chim. Acta* **2003**, *86*, 1063–1084.  
 [15] a) A. Warshel, R. M. Weiss, *J. Am. Chem. Soc.* **1980**, *102*, 6218–6226; b) A. Warshel, *Acc. Chem. Res.* **1981**, *14*, 284–290.  
 [16] J. H. van Lenthe, G. G. Balint-Kurti, *Chem. Phys. Lett.* **1980**, *76*, 138–142.  
 [17] a) P. C. Hiberty, J. P. Flament, E. Noizet, *Chem. Phys. Lett.* **1992**, *189*, 259–265; b) P. C. Hiberty, S. Humbel, J. H. van Lenthe, C. P. Byrman, *J. Chem. Phys.* **1994**, *101*, 5969–5976; c) P. C. Hiberty, S. Shaik, *Theor. Chem. Acc.* **2002**, *108*, 255–272.  
 [18] a) W. Wu, L. Song, Z. Cao, Q. Zhang, S. Shaik, *J. Phys. Chem. A* **2002**, *106*, 2721–2726; b) L. Song, W. Wu, Q. Zhang, S. Shaik, *J. Comput. Chem.* **2004**, *25*, 472–478; c) Z. Chen, J. Song, S. Shaik, P. C. Hiberty, W. Wu, *J. Phys. Chem. A* **2009**, *113*, 11560–11569.  
 [19] P. C. Hiberty, S. Shaik, *J. Comput. Chem.* **2007**, *28*, 137–151.  
 [20] J. H. van Lenthe, J. Verbeek, *J. Mol. Struct. THEOCHEM* **1991**, *229*, 115–137.  
 [21] a) L. Song, Z. Chen, F. Ying, J. Song, X. Chen, P. Su, Y. Mo, Q. Zhang, W. Wu, *XMVB 2.1: An ab initio Non-orthogonal Valence Bond Program*, Xiamen University, Xiamen, **2015**; b) L. Song, Y. Mo, Q. Zhang, W. Wu, *J. Comput. Chem.* **2005**, *26*, 514–521; c) Z. Chen, X. Chen, W. Wu, *J. Chem. Phys.* **2013**, *138*, 164120.  
 [22] F. Penotti, J. Gerratt, D. L. Cooper, M. Raimondi, *J. Mol. Struct. THEOCHEM* **1988**, *169*, 421–436.  
 [23] a) S. S. Shaik, *J. Am. Chem. Soc.* **1981**, *103*, 3692–3701; b) S. S. Shaik, A. Pross, *J. Am. Chem. Soc.* **1982**, *104*, 2708–2719; c) S. Shaik, A. Shurki, *Angew. Chem. Int. Ed.* **1999**, *38*, 586–625; *Angew. Chem.* **1999**, *111*, 616–657; d) See a story of the renaissance of VB theory in: S. Shaik, *Comput. Theor. Chem.* **2017**, *1116*, 2–21.  
 [24] W. Wu, H. Zhang, B. Braïda, S. Shaik, P. C. Hiberty, *Theor. Chem. Acc.* **2014**, *133*, 1441.  
 [25] a) C. Edmiston, K. Ruedenberg, *Rev. Mod. Phys.* **1963**, *35*, 457; b) S. F. Boys in *Quantum Theory of Atoms, Molecules, and the Solid State* (Ed.: P.-O. Löwdin), Academic Press, New York, **1968**, p. 253; c) T. A. Albright, J. K. Burdett, M. H. Whangbo, *Orbital Interactions in Chemistry*, 2nd ed., Wiley, Hoboken, **2013**.  
 [26] a) P. C. Hiberty, C. Leforestier, *J. Am. Chem. Soc.* **1978**, *100*, 2012–2017; b) P. C. Hiberty, G. Ohanessian, *J. Am. Chem. Soc.* **1982**, *104*, 66–70.  
 [27] a) K. Ruedenberg, M. W. Schmidt, M. M. Gilbert, S. T. Elbert, *Chem. Phys.* **1982**, *71*, 41–49; b) K. Ruedenberg, M. W. Schmidt, M. M. Gilbert, *Chem. Phys.* **1982**, *71*, 51–64; c) T. Thorsteinsson, D. L. Cooper, J. Gerratt, P. B. Karadakov, R. Raimondi, *Theor. Chim. Acta* **1996**, *93*, 343–366; d) D. L. Cooper, T. Thorsteinsson, J. Gerratt, *Adv. Quantum Chem.* **1998**, *32*, 51–67; e) D. L. Cooper, P. B. Karadakov, T. Thorsteinsson in *Valence Bond Theory* Ed.: D. L. Cooper, Elsevier, Amsterdam, **2002**, pp. 41–53; f) K. Hirao, H. Nakano, K. Nakayama, M. Dupuis, *J. Chem. Phys.* **1996**, *105*, 9227–9239; g) K. Hirao, H. Nakano, K. Nakayama, *Int. J. Quantum Chem.* **1998**, *66*, 157–175.  
 [28] F. Weinhold, C. Landis, *Valency and Bonding*, Cambridge University Press, Cambridge, **2005**.  
 [29] a) Y. Mo, L. Song, W. Wu, Q. Zhang, *J. Am. Chem. Soc.* **2004**, *126*, 3974–3982; b) Y. Mo, *J. Chem. Phys.* **2003**, *119*, 1300–1306; c) Y. Mo, J. Gao, *J. Phys. Chem. A* **2000**, *104*, 3012–3020; d) Y. Mo, Y. Zhang, J. Gao, *J. Am. Chem. Soc.* **1999**, *121*, 5737–5742; e) Y. Mo, S. D. Peyerimhoff, *J. Chem. Phys.* **1998**, *109*, 1687–1697.  
 [30] “Bridging Cultures”: P. C. Hiberty, S. Shaik in *The Chemical Bond: Fundamental Aspects of Chemical Bonding* (Eds.: G. Frenking, S. Shaik), Wiley, Hoboken, **2014**, pp. 69–90.  
 [31] R. Hoffmann, S. Shaik, P. C. Hiberty, *Acc. Chem. Res.* **2003**, *36*, 750–756.  
 [32] a) W. A. Goddard, T. H. Dunning, Jr., W. J. Hunt, P. J. Hay, *Acc. Chem. Res.* **1973**, *6*, 368–376; b) D. L. Cooper, J. Gerratt, M. Raimondi, *Chem. Rev.* **1991**, *91*, 929–964.  
 [33] A. Grushow, *J. Chem. Educ.* **2011**, *88*, 860–862. See rebuttals in a) D. G. Truhlar, *J. Chem. Educ.* **2012**, *89*, 573–574; b) N. J. Tro, *J. Chem. Educ.* **2012**, *89*, 567–568; c) R. L. DeKock, J. R.

- Strikwerda, *J. Chem. Educ. J. Chem. Ed.* **2012**, *89*, 569; d) C. R. Landis, F. Weinhold, *J. Chem. Educ.* **2012**, *89*, 570–572; e) See Ref. [14a].
- [34] The hybridized lone pairs of H<sub>2</sub>O were the target of virulent attacks, as can be judged by the titles of the articles/book sections: a) *Rabbit-ear hybrids, VSEPR sterics, and other orbital anachronisms*, in: A. D. Clauss, S. F. Nelsen, M. Ayoub, J. W. Moore, C. R. Landis, F. Weinhold, *Chem. Educ. Res. Pract.* **2014**, *15*, 417–434; b) “*Tripods*”, “*rabbit-ears*”, and *other orbital absurdities. Discovering Chemistry with Natural Bond Orbitals* (Eds.: F. Weinhold, C. R. Landis), Wiley, Hoboken, **2012**, p. 68. See Rebuttal in Ref. [14b] above.
- [35] a) T. K. Ghanty, V. N. Staroverov, P. R. Koren, E. R. Davidson, *J. Am. Chem. Soc.* **2000**, *122*, 1210–1214; b) S. J. Grabowski, *Chem. Rev.* **2011**, *111*, 2597–2625; c) M. S. Gordon, J. H. Jensen, *Acc. Chem. Res.* **1996**, *29*, 536–543; d) C. F. Guerra, F. M. Bickelhaupt, E. J. Baerends, *ChemPhysChem* **2004**, *5*, 481–487.
- [36] S. Shaik, P. C. Hiberty, *A Chemist's Guide to Valence Bond Theory*, Wiley, Hoboken, **2008**.
- [37] B. S. Pham, M. S. Gordon, *J. Phys. Chem. A* **2017**, *121*, 4851–4852.
- [38] a) T. Koopmans, *Physica* **1934**, *1*, 104–113; b) O. V. Gritsenko, B. Braïda, E. J. Baerends, *J. Chem. Phys.* **2003**, *119*, 1937–1950.
- [39] K. Jug, P. C. Hiberty, S. Shaik, *Chem. Rev.* **2001**, *101*, 1477–1500.
- [40] a) R. P. Messmer, P. A. Schultz, R. C. Tatar, H.-J. Freund, *Chem. Phys. Lett.* **1986**, *126*, 176–180; R. P. Messmer, *J. Mol. Struct. THEOCHEM* **1988**, *169*, 137–154; P. A. Schultz, R. P. Messmer, *J. Am. Chem. Soc.* **1993**, *115*, 10925–10937.
- [41] a) The preferred conformation of propene was predicted by Pauling, p. 140 of Ref. [2]; b) G. Deslongchamps, P. Deslongchamps, *Org. Biomol. Chem.* **2011**, *9*, 5321–5333; c) G. Deslongchamps, P. Deslongchamps, *Tetrahedron* **2013**, *69*, 6022–6033.
- [42] a) S. Shaik, D. Danovich, W. Wu, H. S. Rzepa, P. C. Hiberty, *Nat. Chem.* **2014**, *4*, 195–200; b) S. Shaik, H. S. Rzepa, R. Hoffmann, *Angew. Chem. Int. Ed.* **2013**, *52*, 3020–3033; *Angew. Chem.* **2013**, *125*, 3094–3109; c) G. Frenking, M. Hermann, *Angew. Chem. Int. Ed.* **2013**, *52*, 5922–5925; *Angew. Chem.* **2013**, *125*, 6036–6039; d) D. Danovich, S. Shaik, R. Hoffmann, H. S. Rzepa, *Angew. Chem. Int. Ed.* **2013**, *52*, 5926–5928; *Angew. Chem.* **2013**, *125*, 6040–6042; e) D. Danovich, P. C. Hiberty, W. Wu, H. S. Rzepa, S. Shaik, *Chem. Eur. J.* **2014**, *20*, 6220–6232; f) G. Frenking, M. Hermann, *Chem. Eur. J.* **2016**, *22*, 4100–4108; g) M. Piris, X. Lopez, J. M. Ugalde, *Chem. Eur. J.* **2016**, *22*, 4109–4115; h) S. Shaik, D. Danovich, B. Braïda, P. C. Hiberty, *Chem. Eur. J.* **2016**, *22*, 4116–4128; i) G. Frenking, M. Hermann, *Chem. Eur. J.* **2016**, *22*, 18975–18976; j) S. Shaik, D. Danovich, B. Braïda, P. C. Hiberty, *Chem. Eur. J.* **2016**, *22*, 18977–18980.
- [43] R. Zhong, M. Zhang, H. Xu, Z. Su, *Chem. Sci.* **2016**, *7*, 1028–1032.
- [44] A. C. West, M. W. Schmidt, M. S. Gordon, K. Ruedenberg, *J. Phys. Chem. A* **2017**, *121*, 1086–1105.
- [45] Y. Liu, T. J. Frankcombe, T. W. Schmidt, *Phys. Chem. Chem. Phys.* **2016**, *18*, 13385–13394.
- [46] a) A. Savin in *Reviews of Modern Quantum Chemistry* (Ed.: K. D. Sen), World Scientific, Singapore, **2002**; b) O. M. Lopes, Jr., B. Braïda, M. Causà, A. Savin in *Progress in Theoretical Chemistry and Physics, Vol. 22* (Eds.: P. E. Hoggan, E. J. Brändas, J. Maruani, P. Piecuch, G. Delgado-Barrio), Springer, Dordrecht, **2012**; c) M. Menéndez, A. M. Pendás, B. Braïda, A. Savin, *Comput. Theor. Chem.* **2015**, *1053*, 142–149.
- [47] For water, see: [http://www.meta-synthesis.com/webbook/45\\_vsepr/VSEPR.html](http://www.meta-synthesis.com/webbook/45_vsepr/VSEPR.html); for ethylene, see Ref. [46].
- [48] G. Acke, S. De Baerdemacker, P. W. Claeys, M. Van Raemdonck, W. Poelmans, D. Van Neck, P. Bultinck, *Mol. Phys.* **2016**, *114*, 1392–1405.
- [49] a) K. Artmann, *Z. Naturforsch.* **1946**, *1*, 426; b) A. Scemama, M. Caffarel, A. Savin, *J. Comput. Chem.* **2007**, *28*, 442–454; c) A. Lüchow, R. Petz, *J. Comput. Chem.* **2011**, *32*, 2619–2626; d) A. Lüchow, *J. Comput. Chem.* **2014**, *35*, 854–864.
- [50] J. H. van Vleck, A. Sherman, *Rev. Mod. Phys.* **1935**, *7*, 167–228.
- [51] See for instance: a) F. M. Bickelhaupt, E. J. Baerends in *Rev. Comput. Chem. Vol. 15* (Eds.: K. B. Lipkowitz, D. B. Boyd), Wiley-VCH, New York, **2000**, pp. 1–86; b) L. P. Wolters, F. M. Bickelhaupt, *WIREs Comput. Mol. Sci.* **2015**, *5*, 324–343.

Manuscript received: September 29, 2017

Accepted manuscript online: December 12, 2017

Version of record online: March 2018, 22